Science Advances
AAAS

advances.sciencemag.org/cgi/content/full/6/45/eaax9538/DC1

Supplementary Materials for

The peripheral effect of direct current stimulation on brain circuits involving memory

Sven Vanneste*, Anusha Mohan, Hye Bin Yoo, Yuefeng Huang, Alison M. Luckey, S. Lauren McLeod, Michel N. Tabet, Rimenez R. Souza, Christa K. McIntyre, Sandra Chapman, Ian H. Robertson, Wing Ting To

*Corresponding author. Email: sven.vanneste@tcd.ie

Published 4 November 2020, *Sci. Adv.* **6**, eaax9538 (2020)
DOI: 10.1126/sciadv.aax9538

This PDF file includes:

Supplementary methods

Experiment 1

Saliva Collection

The length of time to collect 2 ml of saliva was noted and the timer was started only when participants began to passively drool into the tube. The flow rate was calculated using the formula given by Salimetrics: $rate\left(\frac{ml}{min}\right) = \frac{amount\ of\ saliva\ (ml)}{time\ (min)}$. This flow rate correction was used in the calculation of concentration of salivary α-amylase (sAA). Furthermore, the tubes were also weighed; the weight of the saliva was determined as the difference between the weights of the full tube and the empty tube.

Upon completion of the collection procedures, a total of 80 saliva samples were packed in dry ice and sent to the Salimetrics laboratory for analysis. The Salimetrics analysis protocols and determination techniques for each of the two-targeted biomarkers are described below.

The amount of sAA in the sample is directly proportional to the increase in absorbance at 405 nm. 10 µl of the sample is diluted and well mixed. 8 µl of the diluted samples are then pipetted into individual wells of 96-well microtiter plate. 320 µl of preheated chromogenic substrate solution is added to each well and the plate is rotated at 500–600 RPM at 37 C for three minutes. Optical density of the sample is determined at the one-minute mark and again at the three-minute mark.

Electrophysiological recordings

In this experiment, the stimuli were presented binaurally using Sennheiser headphones at 72 dB SPL using the Neuroscan Stim 2 system. The stimuli consisted of 60-ms-duration sinusoidal tones with a 5-ms rise-fall time. The stimuli were divided into two types: 500 Hz (standard) and 1000 Hz (deviant) tones. The deviants constituted 20% of the total presentation. The stimuli were presented with a random interstimulus interval (ISI) of 700–1000 ms with 125 deviant

tones and 500 standard tones. The total duration of the task was anywhere between 8–11 minutes, depending on the ISI. Participants were seated upright and comfortably in a chair in a soundproof room with ambient lighting. They were instructed to press a button every time they heard a high frequency deviant tone while ignoring the presentation of the low frequency standard tones.

The two eye electrodes and bilateral mastoid electrodes were not used during data collection and hence these four channels were removed during preprocessing. The preprocessing pipeline included removing of disconnected and unused channels, re-referencing to an average reference, and band pass filtering between 53–55 Hz. Data from these electrodes were then subject to temporal independent component analysis (ICA) using an infomax algorithm(*53*) in which muscle artifacts, eye blinks, saccades, and other noise transients were removed.

The data were then baseline corrected 100 ms pre-stimulus presentation and were epoched between -100 to +700 ms relative to the stimulus presentation. Artifact detection using a simple voltage threshold of ±90 μV was applied to all epochs. Those epochs that did not fall within this threshold were excluded. The removed channels were then interpolated using a spherical interpolation algorithm in EEGLAB to ensure that all participants had 64 channels of data. Finally, to eliminate the effects of false alarms, only those epochs to which the participants had correctly responded were used for further analysis.

Experiment 2

For the EEG processing, the data were resampled to 128 Hz, band-pass filtered (FFT filter) to 2–44 Hz and re-referenced to average reference using EEGLAB. The data was then plotted in EEGLAB for a careful inspection of artifacts and all episodic artifacts suggestive of eye blinks, eye movements, jaw tension, teeth clenching, or body movement were manually removed from the EEG stream. An artifact was defined as an EEG characteristic that differs

from signals generated by activity in the brain. 1) Some artifacts are known to be in a limited frequency range, e.g., above some frequency. These were removed by frequency filtering. 2) Some artifacts consist of discrete frequencies such as 50 Hz (or 60 Hz for USA) or its harmonics. These were removed by notch filtering. 3) Some artifacts are limited to a certain time range, e.g., in the case of eye blinks. These artifacts were recognized by visual inspection and these time intervals were discarded. 4) Some artifacts originate from one or a few distinct sources or a limited volume of space so that the artifact topography is a superposition of characteristic topographies (equivalently, the artifact is limited to a subspace of the signal space). We removed these artifacts by determining the characteristic topographies (equivalently, the artifact subspace) so that the remaining signals do not contain anything from the artifact subspace. 5) Artifacts and true brain signals that can be assumed to be sufficiently independent can be removed by independent component analysis. 6) Some artifacts are characterized by a particular temporal pattern such as exponential decay. We removed these artifacts by modeling the artifact and fitting its parameters to the data and then removing the artifact. After artifact rejection, a comparison was made between the different groups for the average length of the EEG. This analysis showed no significant differences between the different groups ($F = .34$, $p = .71$). These preprocessing steps were different from the study 1, where we collected ERP data, due to the specific recommendation for source reconstruction and a potential rest-related signal artifact.

Standardized low-resolution brain electromagnetic tomography (sLORETA) was used to estimate the intracerebral electrical sources that generated the scalp-recorded activity in each of the five EEG frequency bands: delta (2–3.5 Hz), theta (4–7.5 Hz), alpha (8–12 Hz), beta (12.5–30 Hz), and gamma (30.5–44 Hz). sLORETA computes electrical neuronal activity as current density (A/m^2) without assuming a predefined number of active sources. The sLORETA solution space consists of 6239 voxels (voxel size 5x5x5 mm) and is restricted to cortical gray

matter and hippocampi, as defined by the digitized Montreal Neurological Institute (MNI) 152 template(*54*). Scalp electrode coordinates on the MNI brain are derived from the international 10-20 system(*55*). The Tomography sLORETA has received validation from studies combining LORETA with other more established methods such as fMRI(*56*), structural MRI(*57*) and PET(*58*). In the current implementation of sLORETA, computations were made in a realistic head model(*54*) using the MNI 152 template(*59*) with the three-dimensional solution space restricted to cortical gray matter. The standard electrode positions on the MNI 152 scalp were taken from (*55, 60*). The intracerebral volume was then partitioned into 6239 voxels at a 5 mm spatial resolution (i.e. the sLORETA solution space). Thus, sLORETA images represent the standardized electrical activity at each voxel in neuroanatomic MNI space as the exact magnitude of the estimated current density. Anatomical labels, as Brodmann areas, are also reported using MNI space. We did not include subcortical regions for our source reconstruction as this modeling is still under discussion especially for regions that are assumed to contribute very weakly to EEG (*61*). In addition, this modeling is mainly applied using MEG data that including more sensors paired with T1weighted MRI volume data (*61*).

Theta–gamma coupling (e.g. by nesting) is proposed to be an effective manner of communication between cortically distant areas(*62*). To verify whether this theta–gamma nesting is present, nesting was calculated for the auditory cortex, the somatosensory cortex, the motor cortex, and the right hippocampus using phase–amplitude cross-frequency coupling. Phase–amplitude was chosen over power–power cross-frequency coupling as the former has been shown to reflect a physiological mechanism for effective communication in the human brain(*62*). Nesting was computed as follows: first, the time-series for the x, y, and z components of the sLORETA current for each ROI was obtained. Next, these were bandpass filtered in the theta (4-7.5 Hz), and gamma (30.5-44 Hz) ranges. These components are the time-series of the electrical current in the three orthogonal directions in space. In each frequency band and for

each ROI, a principal component analysis was computed, and the first component was retained for the theta and gamma bands. The Hilbert transform was then computed on the gamma component and the signal envelope retained. Finally, the Pearson correlation between the theta component and the envelope of the gamma component was computed for each individual (*63, 64*).

Experiment 3

MR images were preprocessed using Statistical Parametric Mapping (SPM12b, Wellcome Department of Imaging Neuroscience, University College London, UK). Images from the first five TRs in the beginning of each session were discarded. We normalized high-resolution structural images to standard MNI template, and segment for three structural components, which were gray matter, white matter, and cerebrospinal fluid. Functional images were realigned to the middle volume to correct for motion artifacts. Slice-timing correction was adjusted for temporal discrepancies between z-direction slices acquired in interleaved manner. After co-registration of functional volumes to the structural image (T1), volumes that contain extreme movements were linearly regressed out as covariates using Artifact Detection Tool (Gabrieli Lab, MIT, US, http://www.nitrc.org/projects/artifact_detect/). Functional images were normalized to the standard template using nonlinear transformation parameters acquired by the process of normalizing structural image to the standard template(*65*). The normalized functional images were smoothed using 6 mm Gaussian kernel.

After preprocessing, the images were processed to account for motion-related and physiological noises using independent component analysis. Confounding factors of signals from white matter and cerebrospinal fluid were linearly regressed out from the global average brain signal using CompCor(*66*). Global signal regression was performed using the grand averaged signal from the gray matter volume. When removing confounding effect, the signal

was simultaneously filtered from 0.01 to 0.17 Hz, where the maximum detectable frequency of the signal is 0.167 Hz (TR = 3 seconds).

Supplementary table 1. Brain regions for the rsfMRI study

	Cluster size	T-value	Peak coordinate		
			x	y	z
During ON-tES: active vs. sham correct for baseline (before ON-tES)					
right temporoparietal junction	1125	34.18	48	-56	3
right mid-cingulate cortex	960	18.14	14	-10	34
left temporoparietal junction	912	20.24	-25	-70	3
right dorsal anterior cingulate	734	20.11	16	30	6
After ON-tES: active vs. sham correct for baseline (before ON-tES)					
right thalamus	1140	31.31	12	-12	16
right dorsolateral prefrontal cortex	713	49.53	26	20	60
left dorsolateral prefrontal cortex	703	33.18	-14	26	54
right superior parietal	677	33.36	40	-58	64
left precuneus	302	20.20	-6	-66	34
left mid-frontal cortex	243	24.49	-48	24	40
right precuneus	220	77.25	29	-16	-15
left somatosensory	129	41.71	-48	-12	62
left mid-temporal cortex	115	19.14	-54	-50	-4
right angular gyrus	76	20.18	52	-54	32
left inferior frontal cortex	73	20.66	-58	30	2
right hippocampus	49	19.60	32	-28	9
right auditory cortex	40	37.77	70	-28	14

FDR-corrected for multiple comparisons ($P < 0.05$)
Coordinates reported in MNI space

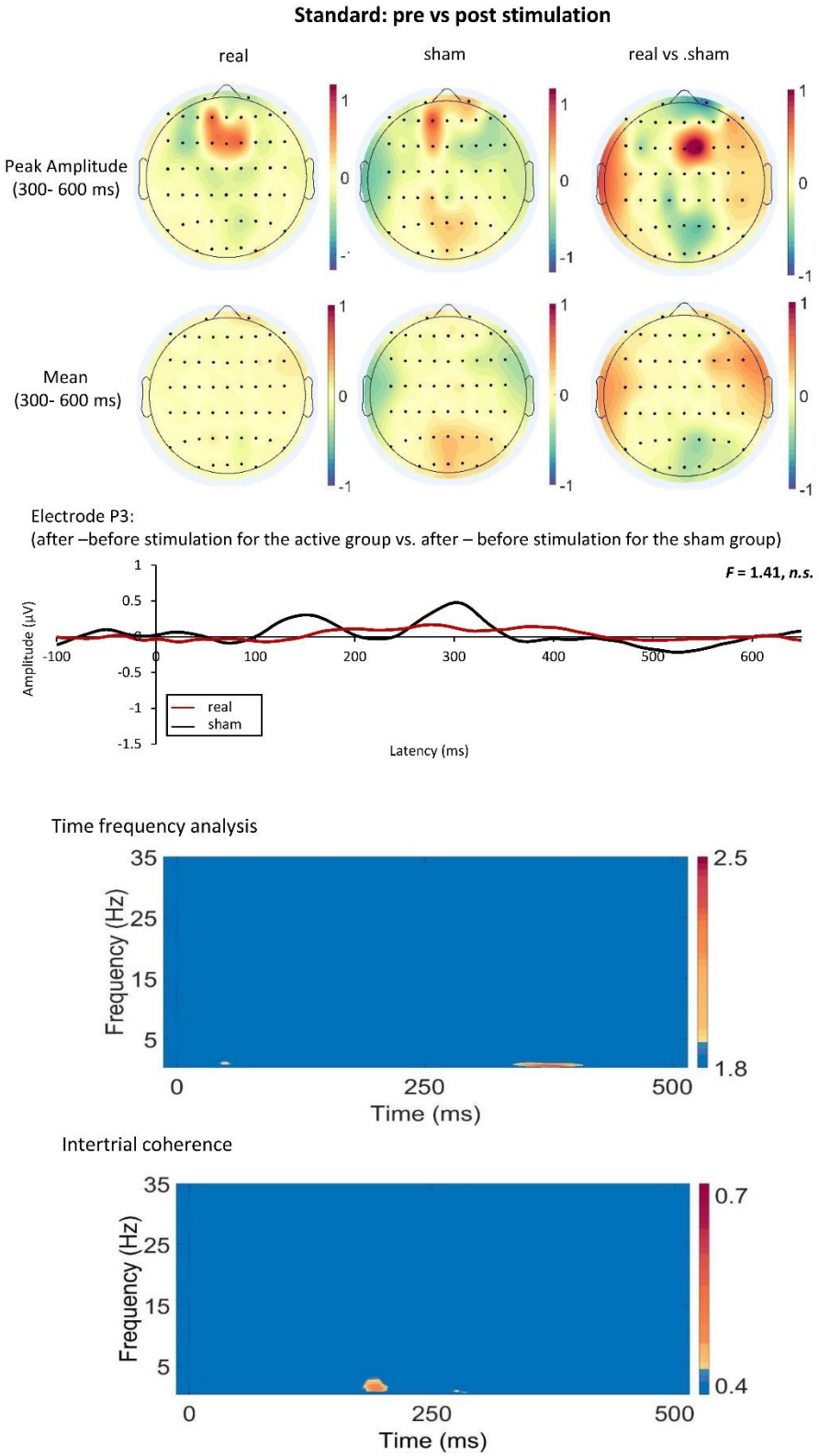

Supplementary figure 1. Neurophysiology for the standard tone of the auditory oddball. Top panel. A comparison between the active group and the sham group after ON-tES does not show a significant effect for the peak amplitude and mean amplitude over 300–600 ms. Middle panel. For the task irrelevant stimuli (standard), we do not see a significant difference between active and sham groups between 300–600 ms as expected ($F_{1,351} = 1.41$, $p = .63$). Bottom panel. A time-frequency analysis for the standard tones and intertrial coherence for the auditory oddball task does not demonstrate any changes after active ON-tES relative to sham ON-tES.

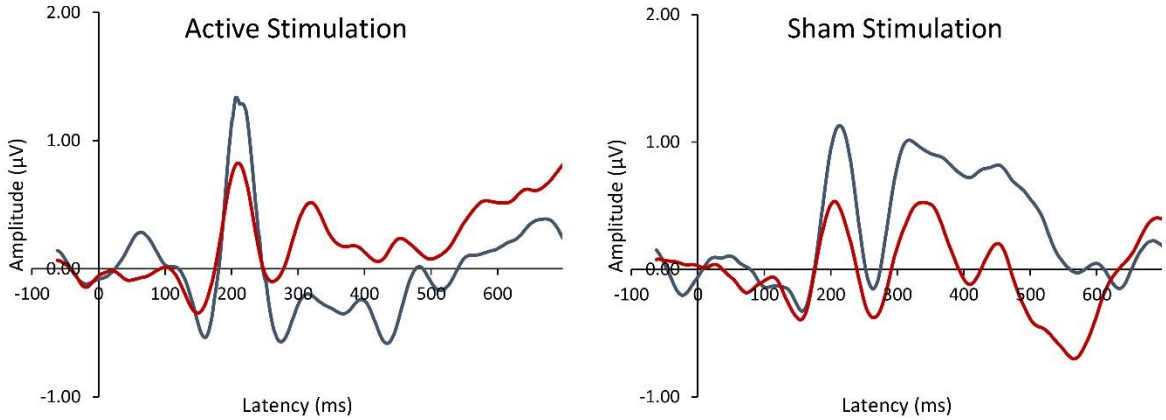

Supplementary figure 2. Representing the ERP signal for the active and sham group separately before and after stimulation

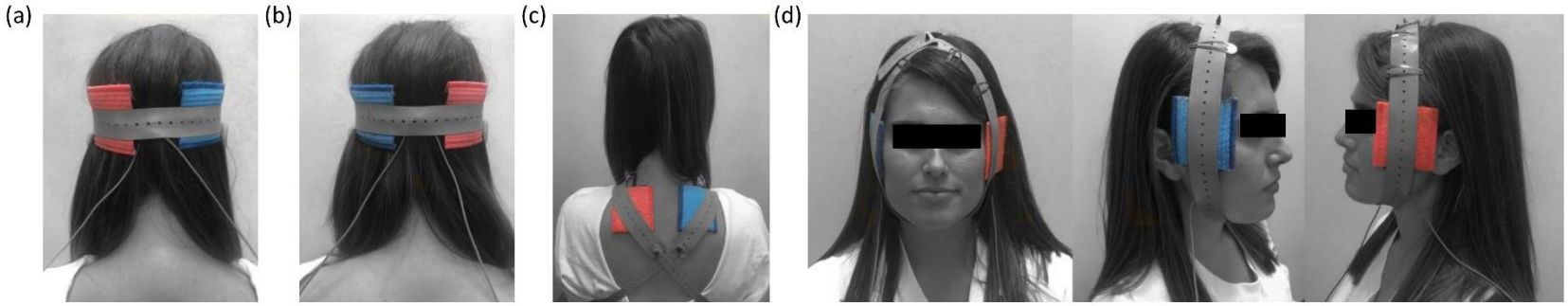

Supplementary figure 3. ON-tES setup for the different experiments. (a) ON-tES with the anode left and cathode right (experiments, 1, 2, 3, 4, 5, 6, 8, 9, 10) (b) ON-tES with the cathode left and anode right (experiment 6) (c) TES targeting the 5-6 occipital nerve with the anode left and cathode right (experiment 6). (d) TES targeting the mandibular nerve of the trigeminal nerve with the anode left and cathode right (experiment 6). Photo credit: Brenda Villasana, UT Dallas.

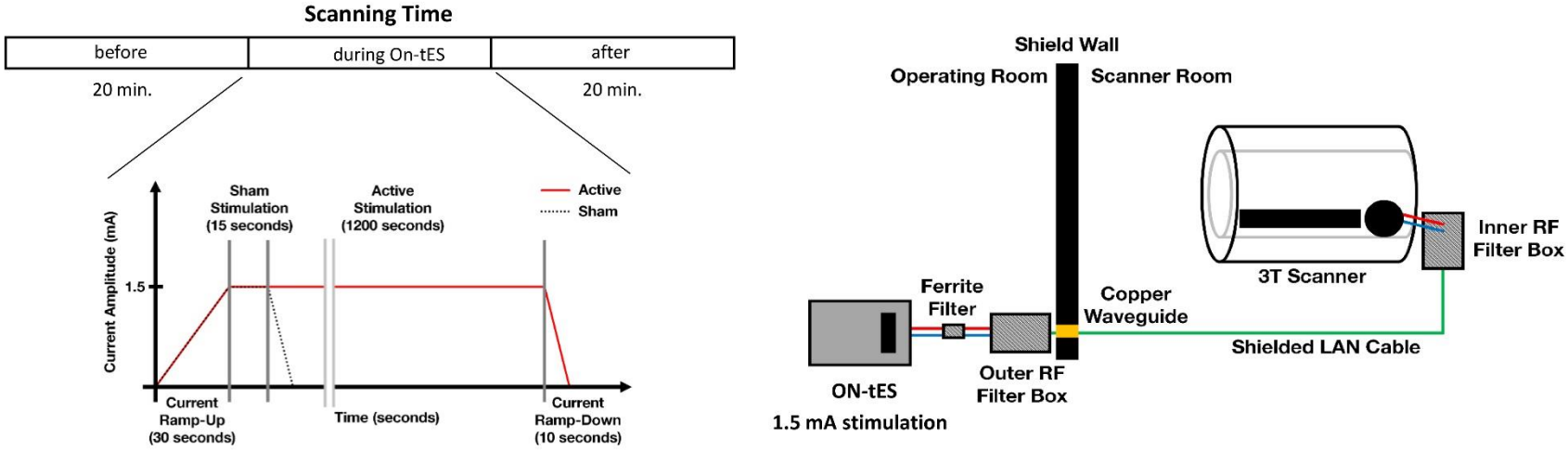

Supplementary figure 4. The left panel shows the study design and the ON-tES design. The right panel shows the setup of the ON-tES with the scanner.